Interfacing Techniques for Time-Domain and Frequency-Domain Simulation Methods

IEEE Task Force on Interfacing Techniques for Simulation Tools
Jose de Jesus Chavez, Abner I. Ramirez, Venkata Dinavahi, Reza Iravani, Juan A. Martinez, Juri Jatskevich, and Gary W. Chang

***Abstract*—This paper reviews different methodologies for interfacing time-domain and frequency-domain simulation programs. The main objective for this interface is to obtain the steady-state or transient state of a power network containing linear and nonlinear loads, and the calculation of the corresponding harmonics and the foregoing values for different types of analyses in power systems.**

***Index Terms*—Frequency-domain analysis, harmonic analysis, interfacing, power system simulation, time-domain analysis.**

I. Introduction

POWER system networks can be computationally solved based on time-domain (TD) and frequency-domain (FD) methods. The former is preferred in cases where switching devices and nonlinear elements are to be considered. The latter is adopted as a standard method in cases where the frequency dependence of the electrical elements is important, or when only (frequency) data measurements are available. Moreover, the refinement of Fourier methods, such as the numerical Laplace transform, has contributed to efficient error control algorithms.

From the implementation point of view, one of the main differences between TD and FD is that the former is based on a sequential solution scheme, allowing iterations within a time step, while the latter is based on a parallel scheme of solution accounting for the whole simulation time at once. Topological changes in the network can be easily incorporated in the TD methodology due to its intrinsic sequential scheme of solution.

In general a power network is composed of both linear and nonlinear elements. The increasing number of switching devices and nonlinear elements demands that a simulation of the power network considers the characteristics of all elements. In this respect, it is desirable that the frequency dependence of a group of network elements be combined with the accurate response of nonlinear time-varying elements. Therefore, there is a need for a hybrid method that can combine the merits of both FD and TD methods for accurate and efficient simulation of power system networks.

Theoretically it is not possible to interface TD and FD due to the differences mentioned above. However, the modeling of a system via its decomposition into external and internal (study) zones, enables such interfacing possible through a transmission line used as a link between the TD and FD parts.

To obtain an efficient hybrid procedure it is recommended that the specific characteristics of TD and FD be considered to decide the parts of the simulation that should be conducted in FD, or TD.

The theory of wavelets, combined with Fourier transform and the dynamic harmonic domain (DHD) provide alternative techniques to deal with the time and the frequency domains simultaneously. These techniques also have been applied for the determination of harmonics in the transient state.

This paper is intended to present a summary of techniques where TD and FD are used simultaneously within the same solution algorithm. The techniques in the literature for interfacing TD and FD algorithms can be broadly classified into three groups (a more detailed description is given in the following sections): (a) Full solution of the network in FD, and conversion of the resultant FD variables to the TD, (b) iterative methods, going back and forth from FD to TD, and (c) solution in TD and FD simultaneously, accounting that the variables depend on both frequency and time.

The paper is organized as follows. Section II describes the general terms and definitions related to the interfacing methodologies. We briefly present the latest definitions reported in the IEEE Standards and the Task Force publications. Section III presents the classical FD techniques used in electrical power systems. Section IV contains the classification of hybrid procedures, and in Section V, the DHD and wavelet techniques are presented. Section VI shows a brief comparison of the hybrid techniques arranged in a table. The conclusions are presented in Section VII.

II. General Terms and definitions

A. Time and Frequency Domains

To analyze the dynamic behavior of an electrical power system, the network components must be represented by a set of equations based on time or frequency as the independent variables. According to the IEEE Standard Dictionary [1]:

Time domain: A function in which the signals are represented as a function of time.

Manuscript received July 01, 2009. First published February 02, 2010; current version published June 23, 2010. Paper no. TPWRD–00459-2009.

The Task Force on Interfacing Techniques for Simulation Tools is with the Working Group on Modeling and Analysis of System Transients Using Digital Programs, IEEE Power and Energy Society Transmission and Distribution Committee. Task Force Chair: V. Dinavahi, Task Force members: U. Annakkage, G. W. Chang, J. Chavez, S. Filizadeh, A. M. Gole, R. Iravani, J. Jatskevich, A. J. Keri, P. Lehn, J. Mahseredjian, J. A. Martinez, B. A. Mork, A. Monti, L. Naredo, T. Noda, A. Ramirez, M. Rioual, M. Steurer, and K. Strunz.

Digital Object Identifier 10.1109/TPWRD.2009.2037152

Frequency domain: A function in which frequency is the independent variable.

TD methods cover all the elements in a power system. It is possible to have a straightforward representation of nonlinear and time varying elements with a very conservative CPU-time and processing memory. Mature and universal time-domain simulation software programs include but are not limited to ATP, PSCAD/EMTDC and EMTP-RV.

On the other hand, FD is intrinsically a linear methodology. It is basically used to model elements with distributed and frequency-dependent parameters. The commonly used FD techniques in power systems are based on the Fourier transform, the numerical Laplace transform and the z-transform.

The maximum frequency for a given network representation is related to the simulation time step through the Nyquist criterion.

B. Interface

An interface is the link between two or more elements, or methodologies. The IEEE Standard Dictionary defines interface data transmission as [1]:

A concept involving the specification of the interconnection between two equipment or systems. The specification includes the type, quantity, and function of the interconnection circuits and the type and form of signals to be interchanged by these circuits.

C. Orthogonality

FD techniques involving the orthogonality property (i.e., two functions $\phi_n(t)$ and $\phi_m(t)$) are said to be orthogonal over the interval $0 < t < T_o$, if the following basic property is satisfied [2]:

$$\int_0^{T_o} \phi_n(t)\phi_m(t)dt \begin{cases} = 0 & \forall n \neq m \\ \neq 0 & \forall n = m. \end{cases} \tag{1}$$

III. Frequency-Domain Techniques

Although the FD analysis is inherently a linear methodology, it can be extended for analyzing nonlinear problems found in power systems. The FD analysis properties that make it attractive are as follows.

- Modeling of network elements with distributed and frequency-dependent parameters can be done rigorously [59].
- Circuit parameters often are obtained and specified in the frequency domain.
- Numerical error levels of the FD computations can be determined and controlled in a straightforward manner [42].
- Being based on principles different to those of the TD methods, the FD analysis constitutes an ideal cross-check for the TD modeling [44].

Some of the classical FD techniques used in power systems and their definitions will be described. Alternate FD techniques, such as Hanker and Mellin transforms (used in signal processing), are not listed here.

A. Fourier Transform

The Fourier Transform and its inverse are defined as follows [3]:

$$F(\omega) = \int_{-\infty}^{\infty} f(t)e^{-j\omega t}dt, \tag{2a}$$

$$f(t) = \frac{1}{2\pi}\int_{-\infty}^{\infty} F(\omega)e^{j\omega t}d\omega. \tag{2b}$$

Analytical solutions are rarely available for practical transient problems. Therefore, one has to resort to numerical solutions by means of discretization of (2a) and (2b). For instance, (2b) can be solved numerically by using three steps as follows.

Step 1) The infinite integration range has to be truncated to a finite value $[-\Omega/2, +\Omega/2]$.

Step 2) $F(\omega)$ has to be sampled within the truncated range at N evenly spaced intervals of length $\Delta\omega = \Omega/N$.

Step 3) Time t is discretized by sampling $f(t)$ inside the range $[0, T]$ at intervals of duration Δt.

Then, the numerical discretization of (2) leads us to the direct discrete Fourier transform (DFT) and the inverse discrete Fourier transform (IDFT) represented by

$$F_m = \sum_{n=0}^{N-1} f_n e^{-j2\pi nm/N},\ m=0,1,2,\ldots,N-1, \tag{3a}$$

$$f_n = \frac{1}{N}\sum_{m=-N/2}^{N/2-1} F_m e^{j2\pi mn/N},\ n=0,1,2,\ldots,N-1. \tag{3b}$$

The fast Fourier transform (FFT) is an algorithm that solves the DFT in a highly efficient manner especially when the number of samples N can be expressed as an integer power of 2. The same applies for the inverse fast Fourier transform (IFFT).

It is mentioned here that once the system has been solved in the FD, the conversion of the solution variables is made through (3b). Note that the TD resolution is related to $\Delta\omega$.

B. Hartley Transform

The Hartley transform [4] has many of the basic properties of the Fourier transform, however, the former handles purely real variables. The Hartley transform application in power systems can be founded in [5], [6]. The Hartley transform of a time function $f(t)$ and its inverse are given by

$$H(\nu) = \int_{-\infty}^{\infty} f(t)cas(\nu t)dt, \tag{4a}$$

$$f(t) = \frac{1}{2\pi}\int_{-\infty}^{\infty} H(\nu)cas(\nu t)d\nu \tag{4b}$$

where $cas(\nu t) = \cos(\nu t) + \sin(\nu t)$ and $\nu = 2\pi f$ are in radians per second.

Similar to the DFT, the discrete Hartley transform (DHT) and its inverse (IDHT) are given by

$$H_m = \frac{1}{N}\sum_{n=0}^{N-1} f_n cas(nm2\pi/N), \quad m = 0,1,2,\ldots,N-1, \tag{5a}$$

$$f_n = \sum_{m=0}^{N-1} H_m cas(nm2\pi/N), \quad n = 0,1,2,\ldots,N-1. \tag{5b}$$

Similarly, the fast Hartley transform (FHT) has been defined to require $(1/2)N\log_2 N$ operations [6]. The system is solved in TD, the conversion of the solution variables is made through (5b). Computationally, the Hartley transform becomes attractive over Fourier-based methods since it handles only real variables [12].

C. Laplace Transform

Let $f(t)$ be a transient waveform and $F(s)$ be its FD image. These functions are related by the Laplace transform and its inverse by [2]

$$F(s) = \int_0^{\infty} f(t)e^{-st}dt, \tag{6a}$$

$$f(t) = \frac{1}{2\pi j}\int_{c-j\infty}^{c+j\infty} F(s)e^{st}ds \tag{6b}$$

where s is the complex frequency $s = c + j\omega$; ω corresponds to the angular frequency variable and c is a positive real damping constant. Alternately, (6a) and (6b) can be expressed as [7]

$$F(s) = \int_0^{\infty} \left[f(t)e^{-ct}\right] e^{-j\omega t}, \tag{7a}$$

$$f(t) = \frac{e^{ct}}{2\pi}\int_{-\infty}^{+\infty} F(c+j\omega)e^{j\omega t}. \tag{7b}$$

From (7a), it can be noticed that the Laplace transform can be interpreted as the Fourier transform of a signal that has been damped artificially through its multiplication with a decaying exponential function $f(t)e^{-ct}$ [see (2a) and (2b)]. This exponential damping makes the reduction of aliasing errors possible when (7b) is used. In fact, this is the approach of the modified Fourier transform (MFT) [8]–[10].

With $f(t)$ being a real and causal function, the inverse Laplace transform is

$$f(t) = \Re\left\{\frac{e^{ct}}{\pi}\int_0^{+\infty} F(s)e^{j\omega t}d\omega\right\}. \tag{8}$$

The numerical evaluation of (8) requires sampling intervals $\Delta\omega$ and Δt given by (11a) and (11b), respectively. Furtermore, we define

$$f_n \equiv f(n\Delta t), \text{ for } n=0,1,2,\ldots,N-1, \tag{9a}$$

$$F_{2m+1} \equiv F(c+j(2m+1)\Delta\omega), \text{ for } m=0,1,\ldots,N-1, \tag{9b}$$

where for time and frequency domains, we use N equally spaced samples. The observation time T corresponds to the waveform repetition period. In this case, it is

$$T = P_o = 2\pi/(2\Delta\omega) = \pi/(\Delta\omega). \tag{10}$$

Thus, we can establish the following relations:

$$\Delta t = T/N, \tag{11a}$$

$$\Delta\omega = \Omega/2N = \pi/T \tag{11b}$$

where Ω corresponds to the maximum frequency. Using the sampling scheme and the definitions from (9a)–(11b), (8) can be numerically approximated as

$$f_n = \Re\left\{C_n\left[\sum_{k=0}^{N-1} F_{2k+1}\sigma_{2k+1}e^{j2\pi kn/N}\right]\right\} \tag{12}$$

where

$$C_n = 2Ne^{cn\Delta t}e^{j\pi n/N}\Delta\omega/\pi. \tag{13}$$

The term inside the square brackets in (12) permits us to utilize the FFT algorithm [2]. This method is known in the specialized literature as the numerical Laplace transform (NLT).

Similar to the Fourier transform, the numerical Laplace transform permits solving the system in the FD. A subsequent step is to convert all of the FD variables under study to the TD, see (12). In this method, one can notice the strong relation between Δt and $\Delta\omega$. Physically, it means that the faster the transient is, the larger $\Delta\omega$ and the shorter Δt.

D. Walsh Transform

The Walsh functions are a complete, orthogonal set of square wave-like functions defined on the interval [0, 1] [11]. The Walsh series representation of a time function and its inverse are

$$F(m) = \int_0^1 f(t)wal(m,t)dt, \tag{14a}$$

$$f(t) = \sum_{m=0}^{\infty} F(m)wal(m,t). \tag{14b}$$

For the discrete case, the integral of (14a) can be approximated by a summation expression to obtain the discrete Walsh transform (DWT) (14a) and its respective inverse (IDWT) from (14b), as given by [12]

$$F(m) = \frac{1}{N}\sum_{n=0}^{N-1} f(n)wal(m,n), \quad m = 0,1,2,\ldots,N-1, \tag{15a}$$

$$f(n) = \sum_{m=0}^{N-1} F(m)wal(m,n), \quad n = 0,1,2,\ldots,N-1 \tag{15b}$$

where $wal(m,n)$ is the discrete Walsh function corresponding to $wal(m,t)$, $f(n)$ is the nth sampled value of $f(t)$ obtained by sampling $f(t)$ N times during the interval [0, 1], and N is an integer power of 2.

For instance, $wal(m,n)$ for $N = 8$ as a normalized time period, can be represented by

$$wal(m,n) = \begin{bmatrix} 1 & 1 & 1 & 1 & 1 & 1 & 1 & 1 \\ 1 & 1 & 1 & 1 & -1 & -1 & -1 & -1 \\ 1 & 1 & -1 & -1 & -1 & -1 & 1 & 1 \\ 1 & 1 & -1 & -1 & 1 & 1 & -1 & -1 \\ 1 & -1 & -1 & 1 & 1 & -1 & -1 & 1 \\ 1 & -1 & -1 & 1 & -1 & 1 & 1 & -1 \\ 1 & -1 & 1 & -1 & -1 & 1 & -1 & 1 \\ 1 & -1 & 1 & -1 & 1 & -1 & 1 & -1 \end{bmatrix}.$$

For analysis purposes, initially, the system is solved in FD by Walsh series. Then, the solution is found as the superposition of several step responses. Finally, the conversion of the solution variables is made through (15b). The Walsh transform has potential applications in the analysis of truncated waves in electric circuits due to the compactness of the sequence spectrum of these waves. A fast Walsh transform also exists (FWT) that has been efficiently used in the power-quality area [60].

E. Z-Transform

The z-transform [14], is a powerful tool to solve linear, constant-coefficients difference equations. It has both FD and TD properties and can be considered as an FD method due to the close relationship that it has with the Laplace transform.

Based on the Laplace transform, the z-transform can be derived using the one-sided discrete Laplace transform [15], [16]

$$F(s) = \sum_{k=0}^{\infty} f(k\Delta t)e^{-ks\Delta t}. \tag{16}$$

Based on the following definition:

$$z = e^{s\Delta t}, \tag{17}$$

substituting (17) and (16) becomes

$$F(z) = \sum_{k=0}^{\infty} f_k z^{-k}. \tag{18}$$

Equation (18) corresponds to the definition of the one-side z-transform [2].

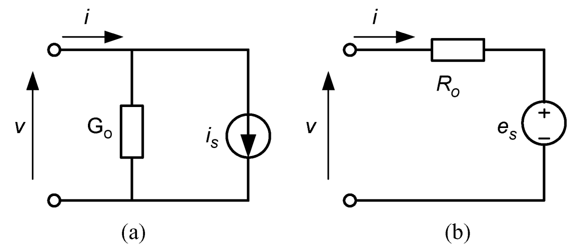

Fig. 1. Norton and Thevenin equivalents circuits for the z transform.

Consider the FD input–output relation of a linear time-invariant system described by

$$Y(s) = H(s)X(s), \tag{19}$$

where $H(s)$ is the transfer function of the system and $X(s)$ and $Y(s)$ are the input and the output, respectively. In most z-transform applications to EMT simulations, the transfer function $H(s)$ is replaced (approximated) by a rational function z^{-1} of the form

$$H(z) = \frac{b_o + b_1 z^{-1} + \cdots + b_N z^{-N}}{1 + a_1 z^{-1} + \cdots + a_N z^{-N}} \tag{20}$$

where the coefficients $a_1, \ldots, a_N, b_o, \ldots, b_N$ are identified by fitting the frequency response of (20) with a given $H(j\omega)$. Alternatively, they can be obtained in the TD by matching the time response of (20) with recorded or calculated data. After identification, substituting (20) into (19) gives

$$(1 + a_1 z^{-1} + \cdots + a_N z^{-N})Y(s) = (b_o + b_1 z^{-1} + \cdots + b_N z^{-N})X(s). \tag{21}$$

By noting that the z^{-1} operator implies a one-sample delay in TD, and using the shift theorem, we obtain

$$y(n) = b_o x(n) + b_1 x(n-1) + \cdots + b_N x(n-N) - a_1 y(n-1) - \cdots - a_N y(n-N). \tag{22}$$

The transformation of (20) to the discrete time domain indicates that the output can be calculated by $2N+1$ multiplications and $2N$ additions, which are very efficient if the model order N is small.

Expression (22) can be rewritten in the form

$$i(n) = G_o v(n) + i_s(n) \tag{23}$$

where v and i are the voltage and the current and

$$G_o = b_o, i_s(n) = \sum_{k=1}^{N} \{b_k v(n-k) - a_k i(n-k)\}. \tag{24}$$

Thus, (23) and (24) can be interpreted as the Norton equivalent circuit shown in Fig. 1(a), which is compatible with the nodal formulation used in Electromagnetic Transients Program (EMTP)-type programs.

Similarly, (22) can be rewritten in the form

$$v(n) = R_o i(n) + e_s(n) \tag{25}$$

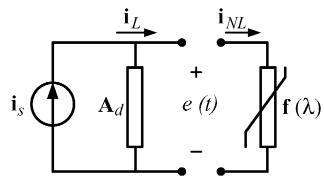

Fig. 2. Steady-state approach: Norton equivalent decomposition into linear and nonlinear subsystems.

where

$$R_o = b_o, e_s(n) = \sum_{k=1}^{N} \{b_k i(n-k) - a_k v(n-k)\}. \quad (26)$$

Thus, (25) and (26) can be interpreted into the Thevenin equivalent circuit shown in Fig. 1(b).

IV. Hybrid TD-FD Methods

Based on the type of power system analysis the hybrid TD-FD methods are classified into three regimes: 1) steady-state, 2) dynamic, and 3) transient. In this section, the basics of the most commonly used methods are described. Applications for most of them are relegated to the references.

A. Steady-State Approach

1) Harmonic Power Flow: Our classification of hybrid methodologies, in the steady-state, start with the harmonic power flow method [17], [18]. This methodology consists in a superposition of the steady-state phasor solutions at the fundamental frequency and at the dominant harmonics frequencies [19]. It can either be used by itself, or as an initialization procedure for the electromagnetic transient studies in a hybrid procedure. Harmonic power flow analysis was primarily developed as an improved initialization procedure for the EMTP, for cases where the initial steady-state was already distorted with the harmonics produced by nonlinear elements. To obtain the steady-state solution in a network, using harmonic power flow, first the nonlinear loads are replaced by voltage-dependent current sources at the fundamental frequency to make the network linear. Second, the voltages at any other frequency are then found by solving a system of nodal equations of the form $\mathbf{YV} = \mathbf{I}$. The solution is deduced in two iterative loops: power flow iterations are used to obtain the solution at the fundamental frequency, while distortion iterations take the higher harmonics into account [20]–[22].

2) Harmonic Balance Type A: Generally power systems networks are divided in two subsystems, one containing linear and frequency dependent elements, the other containing nonlinear elements and switches (Fig. 2). The voltage where the system is partitioned $e(t)$ and/or the flux-linkage (λ), corresponding to the nonlinear element, are assumed to be in the form of a truncated Fourier series. Currents are determined separately for both subsystems as

$$\mathbf{i}_{NL} = \mathbf{f}(\lambda), \quad (27a)$$

$$\mathbf{i}_L = \mathbf{i}_{sc} - IFFT[A_d]FFT[\boldsymbol{\lambda}] \quad (27b)$$

where subscripts L and NL stand for the linear and nonlinear parts, respectively; $\mathbf{f}(\lambda)$ represents the nonlinear load current; A_d is a complex-valued diagonal matrix for the linear network; and $\mathbf{i}_{sc}$ is the current injected by the source into a short circuit at the terminal of the nonlinear element [23], [24].

A Newton–Raphson iterative procedure may be used to determine the desired flux-linkage waveform

$$\boldsymbol{\lambda}^{k+1} = \boldsymbol{\lambda}^k - \left\{\mathbf{J}_h^{-1}\right\}^k \{\mathbf{i}_{NL} - \mathbf{i}_L\}^k \quad (28)$$

where matrix $\mathbf{J}_h$ is

$$\mathbf{J}_h = \mathbf{f}'(\lambda) + IFFT[\mathbf{A}_d] \quad (29)$$

and $\mathbf{f}'(\lambda)$ is a diagonal matrix whose elements are $\partial f(\lambda)/\partial(\lambda)$. The waveform $\boldsymbol{\lambda}$ is adjusted until the mismatch between the two currents is less or equal to a predetermined value corresponding to the steady-state response at the end of the simulation ($\mathbf{i}_{NL} - \mathbf{i}_L = [0]$).

3) Harmonic Balance Type B: The harmonic balance method has been used as a means of analyzing the behavior of harmonic ordinary differential equations (ODEs) [25]. The technique involves assuming a solution in the form of a truncated Fourier series with a predetermined number of harmonics for a network in the steady state [26]. Similar to the Harmonic Balance Type A method, the network is divided in two subsystems, one with linear elements the other with nonlinear elements; the partition is done at the buses where nonlinear loads are connected. Voltage $\mathbf{V}_h$ (Fig. 3) for all harmonics where nonlinear loads are connected is assumed to start the simulation. The underlying idea is based on the calculation of a current mismatch between both subsystems. In the linear part, current $\mathbf{I}_L$ is obtained by using $\mathbf{I}_L = \mathbf{Y}_h\mathbf{V}_h$, where $\mathbf{Y}_h$ is a harmonic matrix representation of all the linear elements [27]. On the other hand, a TD simulation is used to obtain current $i_N(t)$.

It is expected that $\Delta\mathbf{I} = \mathbf{I}_N + \mathbf{I}_L$ will be equal to zero. However, before convergence, $\mathbf{V}_h$ is not yet accurately known, resulting in a current mismatch $\Delta\mathbf{I}$. As seen from the interfacing bus, the system has the admittance $\mathbf{Y}_h$ plus the admittance of the nonlinear part. We can use, as voltage correction $\Delta\mathbf{V}_h$, the solution of the equation

$$\tilde{Y}_h \Delta V_h = \Delta I_h$$

with an appropriate approximation for $\tilde{Y}_h$. The procedure ends when the determined value of $\Delta\mathbf{I}$ is close to zero. Fig. 3 gives a conceptual representation of this procedure. The described procedures present certain advantages against TD methods. One is the computational convergence speed for large networks. Also, nonlinearities can be linearized for harmonic balance-type studies [28].

4) Harmonic Balance Type C: Hybrids methodologies have been used in harmonic distortion studies. The size of equations in harmonic method depends on the number of variables and the harmonic content, thus becoming a computational bottleneck. This method is similar to the Type A and Type B procedures previously described and consists of the following steps:

Step 1) Decomposition of the total network into its linear and nonlinear parts [29], [30].

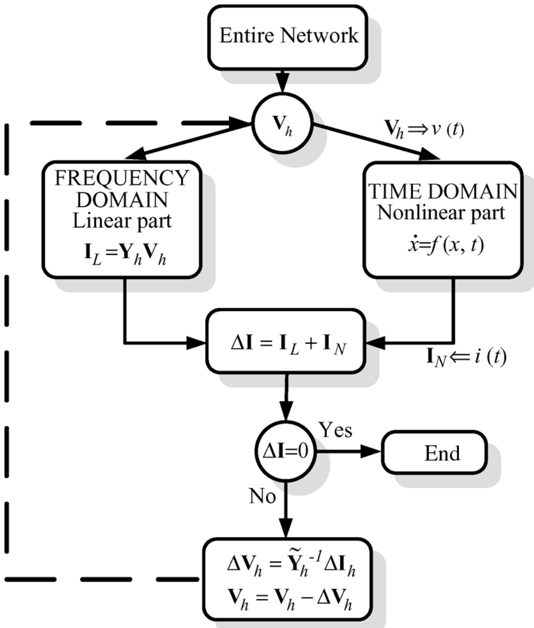

Fig. 3. Harmonic Balance Type B procedure.

Step 2) Modeling the linear network in the FD and computation of a Norton equivalent [31].

Step 3) Computation of harmonic currents injected by the nonlinear devices. This is performed by means of a TD simulation for each device, in which the voltage V_h, is known from the previous iteration. Once the steady-state is deduced for each device, a FFT is performed on the currents absorbed by the nonlinear devices.

Step 4) Formulation and solution of the nonlinear algebraic (30a) with a Newton-Raphson procedure. The mismatch between the two successive iterations is calculated based on (30b)

$$I_{eq} - Y_{eq} V_h = I_{NL}, \tag{30a}$$

$$\varepsilon = max\left|V_h^{k+1} - V_h^k\right|, \tag{30b}$$

where I_{eq} and Y_{eq} correspond to the Norton equivalent of the linear system, I_{NL} is the current from the nonlinear load, and h represents the highest harmonic. If the mismatch in (30b) is smaller than a predefined tolerance, the process is terminated [32], [33].

The harmonic balance method provide the following advantages:

- Computation time and memory space are greatly reduced.
- They can consider linear load unbalances and structural unbalance, and it is possible to represent loads, capacitor banks, or filters with several configurations, connected to ground or isolated.
- Nonlinear loads are modeled in TD, with the greatest flexibility to represent any kind of topology.
- The complex process needed to solve the steady state of an unbalanced network with nonlinear elements is simplified offering good properties of convergence and great flexibility to analyze a variety of systems that can impose difficulties using other methods.

B. Power System Dynamics

1) Transient Stability: To effectively use a hybrid procedure for transient stability analysis, it must be considered if a FD algorithm can be competitive and identified parts (if any) of the simulation that should be conducted in FD as opposed to the TD. According to the traditional method for transient stability analysis and based on the previous sections, linear elements are modeled in FD where it is possible to identify each potentially hazardous oscillation frequency. Nonlinearities, in this case generators, are modeled in TD. The procedure is as follows:

- The classical representation of each generator is given as

$$m_k\ddot{\delta}_k + d_k\dot{\delta}_k + P_{e,k} - P_{m,k} = 0 \tag{31}$$

  where δ is the machine angle, and the subscript k denotes machine k.
- To incorporate the generator signals into the network, the generator voltages are converted from TD to FD, by using a FFT with a relative small window to maintain accuracy

$$\mathbf{V}_k = FFT\left[v_k(t)\right]. \tag{32}$$

- The result is coupled to the network based on

$$\mathbf{YV} = \mathbf{I}, \tag{33}$$

  where $\mathbf{Y}$ is the network admittance matrix including the generators reactances, and $\mathbf{V}$ is the vector of voltages, including the generator voltages.
- IFFT is applied to transform the resulting FD currents back into TD to work with the nonlinear elements

$$i_k(t) = IFFT[\mathbf{I}_k]. \tag{34}$$

The procedure is repeated until the required time is complete. The main advantage of using hybrid TD-FD techniques in transient stability analysis is the reduction of the computational time [35]–[38].

2) Fault Analysis: The methods that combine TD and FD can also be used for the fault analysis [39]–[41] to produce results that are superior to those obtained in the classical fault analysis, without demanding a large increase in the computation time. For such analysis, synchronous machines and induction motor loads are represented in the TD by high-order models that accurately predict the electrical and mechanical responses of the machines. The power system is represented in FD. The algorithm progresses first by solving the source and load model equations to determine the most recent values of each components terminal currents. A least square estimation algorithm is then utilized to convert the differential equation solutions into equivalent FD phasors. It is assumed that at any time the entire history of the differential equations are available and the

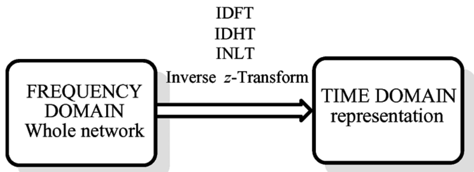

Fig. 4. Electromagnetic transient study: solution in FD, representation in TD.

function is assumed to be a single frequency sinusoid $x(t) = X_c cos(\omega t) + X_s sin(\omega t)$, the coefficients X_c and X_s can be related to the samples assuming a window of three samples, and then are used to estimate magnitude and angle by

$$X_m = \sqrt{X_c^2 + X_s^2}, \tag{35a}$$

$$\phi = \tan^{-1}\left\{\frac{-X_s}{X_c}\right\}. \tag{35b}$$

The currents are used in $\mathbf{YV} = \mathbf{I}$ to obtain the network node voltages. The algorithm should be solved concurrently, but due to the decoupled nature of the methodologies, a simultaneous solution of all equations is not possible. A small time step is used to avoid errors due to time skew.

C. Electromagnetic Transients

1) Full Frequency Domain Solution: FD is widely recommended as a complement to the standard TD analysis tools. Ideal sources and passive elements are modeled using one of the transform methods described in Sections III-A-F [44]–[47]. Representation of basic functions in Fourier, Laplace and z-transform can be found in [2]. The resultant algebraic equations are solved for a specific frequency range [43] and at the end the packed of results is transformed to the TD via an inverse transform of the selected technique. For instance, the numerical inverse Laplace transform from (12) including a window function $\sigma(\omega)$ to reduce truncation errors, is given by

$$f_n = \Re\left\{C_n\left[IFFT(F_2\sigma_2)\right]\right\}. \tag{36}$$

Fig. 4 shows the procedure for calculating a transient event in FD and converting the variables of interest to the TD. These method has also been extended to nonlinear loads and switches [48].

2) Two-Zone Hybrid Solution: As in the steady-state approach, this hybrid procedure partitions the system in two subsystems: one (study zone) is modelled in the TD and the other (external zone) in the FD. The link between them consists on a transmission line [49]. This methodology is briefly explained based on the definitions shows in Fig. 5. First the incident wave voltage at node A, $v_{A,inc}$ is known beforehand and used to calculate the reflected wave voltage $v_{A,refl}$ in the TD, over a time span 2τ. Then, $v_{A,refl}$ is transformed into the FD via an FFT operation to obtain $\mathbf{V}_{A,refl}$, taken as an input for the external zone where $V_{A,inc}$ is computed in the FD by a multiplication of transfer functions as in (37). Finally, $v(t+2\tau)_{A,inc}$ is calculated in the TD through

$$v(t+2\tau)_{A,inc} = IFFT[H_{sh}H_{ex}H_{sh}] \tag{37}$$

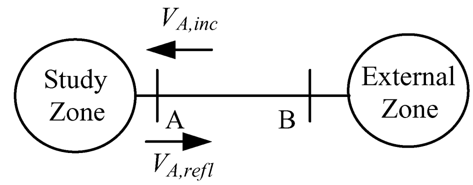

Fig. 5. Basic configuration for the two-zone hybrid solution.

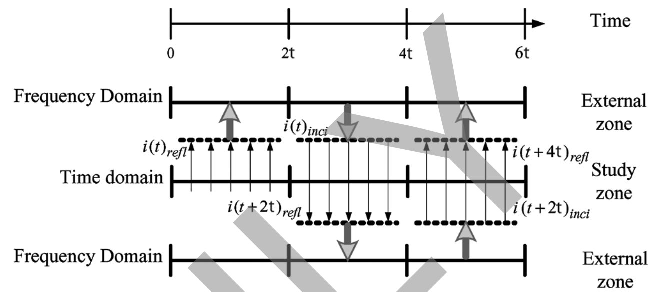

Fig. 6. Two-zone hybrid solution for electromagnetic transient simulation.

where H_{ex} is the external zone transfer function and H_{ex} is the shaping function obtained by the propagation function H_p and the delay, and

$$H_{sh} = e^{j\omega\tau} \times H_p. \tag{38}$$

The procedure just discussed is shown in Fig. 6 and repeated until the required simulation time is complete.

The advantages of this method are that the accuracy and simplicity of the FD modeling are preserved, no approximation or fitting is required, and the resulting accuracy cannot be matched by the "equivalent methods." However, the disadvantage is that the external zone and study zone must be connected by a transmission line with a travel time τ.

3) Hybrid Method for Steady and Dynamic States: This methodology, based on the numerical Laplace transform, has been proposed to calculate electromagnetic transients or to compute the steady state of a network including nonlinear elements [50]. For transient calculations the NLT is applied in its original formulation. In the case of steady state computations a slightly modified NLT is used. Basically, the linear and nonlinear parts of the network are treated separately (see Fig. 7) and a current mismatch for the node joining both subnetworks is defined. Assuming initially a known voltage V_{old}, the current entering the linear part I_L is calculated in the FD where the corresponding Jacobian J_L corresponds to a known admittance-based matrix. On the other hand, the current entering the nonlinear part I_{NL} is calculated in the TD and the calculation of the corresponding Jacobian J_{NL} is calculated numerically via small perturbations to the input (taken as a voltage) at the connecting node. Regarding the nonlinear part, the process of going from FD to TD and vice–versa is made through NLT operations. Joining the two subnetworks in their linearized form (in FD) yields

$$\Delta V = (J_L + J_{NL})\Delta I. \tag{39}$$

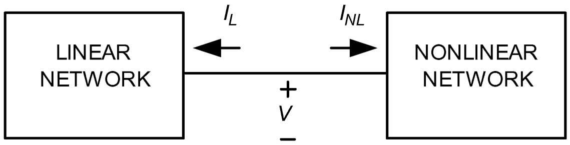

Fig. 7. Representation of the complete network.

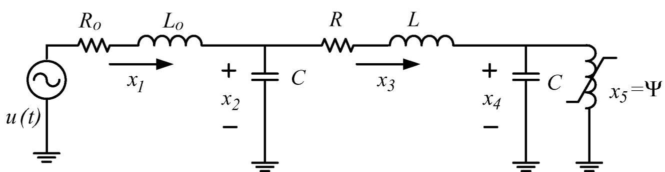

Fig. 8. Nonlinear network.

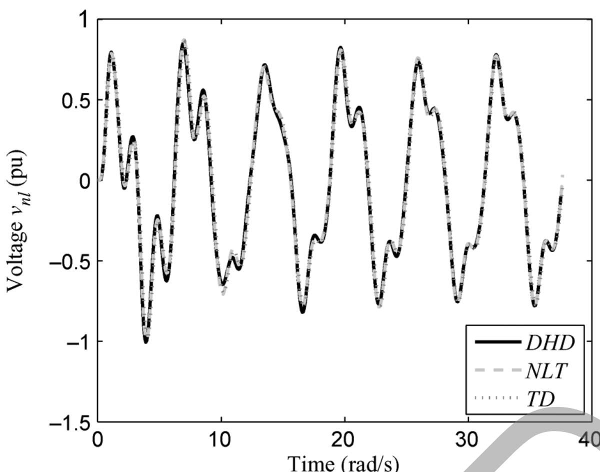

Fig. 9. Voltage across nonlinear load using the DHD, NLT hybrid, and the TD.

Thus, a Newton-type iterative scheme to calculate a new voltage is given by the recursive relation (taking the appropriate signs of the currents)

$$V_{new} = J^{-1}(-\Delta I) + V_{old}. \tag{40}$$

The resulting method is attractive for handling frequency dependent network elements tied to nonlinear loads and possibly including inter harmonics. A major advantage of the proposed method over the existing ones is that there is no need of resorting to iterative methods for solving the nonlinear part of the network. Additionally, a minor modification of the algorithm permits to switch from steady state to transient calculations.

4) Illustrative Example: As an example consider the circuit shown in Fig. 8. It consists of a combination of a source $u(t) = \sin(\omega_o t) + 0.1\sin(3\omega_o t) + 0.05\sin(5\omega_o t)$ with $\omega_o = 1$, $R_o = 0.1$ and $L_o = 0.3$, a lumped parameter transmission line with $R = 0.2$, $L = 0.2$ and $C = 0.2$, and a nonlinear inductance as a load having a current/flux relation given by $i = 1.2\varphi + 0.5\varphi^3$. All of the parameters are in per unit.

The source in the circuit from Fig. 8 is connected at $t = 0$ and the voltage across the nonlinear load is calculated. The voltage is shown in Fig. 9, where we can notice that the three resulting waveforms (labeled TD, DHD and NLT hybrid) are superimposed.

V. Dynamic Harmonic Domain and Wavelet Techniques

Dynamic harmonic domain and wavelets methodologies are able to represent power networks simultaneously in time and frequency domains for dynamic and transient studies.

A. Dynamic Harmonic Domain

The DHD is a direct approach for transient and steady-state solution of harmonics. It is based on orthogonal and operational matrices, with the coefficients of the orthogonal basis being the state variables. Intrinsically, the DHD solution allows the possibility of step-by-step computation of evolution of the harmonic coefficients. In addition, the DHD methodology provides the power-quality (PQ) indices used in steady-state applications as functions of time.

In this section, we describe the conversion of an ODE from TD to the DHD [51]. Without the loss of generality, consider the linear time periodic (LTP) system for the scalar case

$$\dot{x} = a_p x + b_p u, \tag{41a}$$
$$y = c_p x + d_p u \tag{41b}$$

where subscript p stands for time-periodic; for instance,a_p is defined as

$$a(t)_p = a(t)_{-h}e^{jh\omega_o t} + \cdots + a(t)_o + \cdots + a(t)_h e^{jh\omega_o t} \tag{42}$$

with h and ω_o representing the highest harmonic and the fundamental frequency. Expressing all of the variables from (41a) and (41b) by their Fourier series (with time-varying coefficients) and removing all of the exponential factors, the state representation (41a) and (41b) in the DHD becomes [53]

$$\dot{\mathbf{x}} = (\mathbf{A} - \mathbf{S})\mathbf{x} + \mathbf{B}u, \tag{43a}$$
$$\mathbf{y} = \mathbf{C}\mathbf{x} + \mathbf{D}\mathbf{u}, \tag{43b}$$

where the variables are now complex vectors (represented by bold-type letters) with time-varying coefficients, e.g.,

$$\mathbf{x} = [x_{-h}(t), \cdots, x_o(t), \cdots, x_h(t)]^T, \tag{44}$$

where T denotes the transpose. $\mathbf{S}$ is called the operational matrix of differentiation given by [54]

$$\mathbf{S} = diag\{-jh\omega_o, \ldots, -j\omega_o, 0, j\omega_o, \ldots jh\omega_o\} \tag{45}$$

and $\mathbf{A}$ (as well as $\mathbf{B}$, $\mathbf{C}$, and $\mathbf{D}$) has the Toeplitz structure

$$\mathbf{A}(t) = \begin{bmatrix} a_o & a_{-1} & \cdots & a_{-h} & \\ a_1 & a_o & & & a_{-h} \\ \vdots & & \ddots & & \vdots \\ a_h & & & a_o & a_{-1} \\ & a_h & \cdots & a_1 & a_o \end{bmatrix}. \tag{46}$$

Note that in the DHD, we obtain a system of ODEs of dimension $2h+1$ for the general case. The system becomes diagonal when dealing only with linear elements, and can further be reduced to order $h/2$ when considering half-wave symmetry (i.e., only odd harmonics). Note also that if a_p (as well as b_p, c_p, and d_p) from (41a) is a real coefficient (a non-periodic quantity) (46)

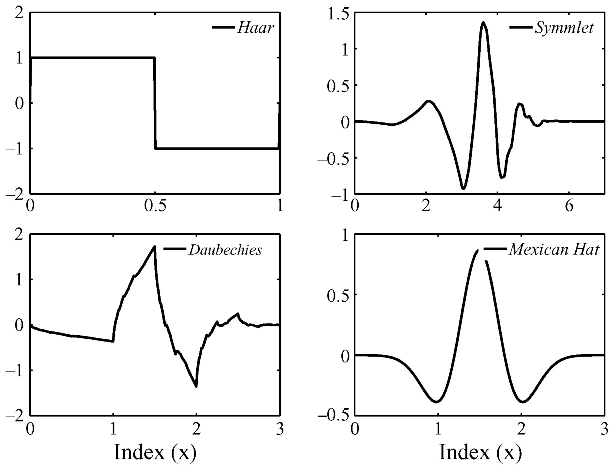

Fig. 10. Classical mother wavelet functions w.

becomes a diagonal matrix. By comparing (41a) and (43a), one can observe that the LTP system has been transformed into a Linear Time Invariant (LTI) system through the DHD. Moreover, the steady-state of the system is easily obtained by setting to zero the derivatives in (43a) yielding [52]

$$\mathbf{x} = (\mathbf{A} - \mathbf{S})^{-1}\mathbf{B}\mathbf{u}, \tag{47a}$$

$$\mathbf{y} = \mathbf{C}\mathbf{x} + \mathbf{D}\mathbf{u}. \tag{47b}$$

The evolution of the harmonic content, with respect to time, can be obtained from (43a) and the corresponding instantaneous values are calculated by assembling a Fourier series as in (42). Potential applications of the DHD technique are in the areas of power-quality studies and analysis of possible ferroresonance conditions.

The accuracy of the DHD results depends on the number of harmonics included in the modeling (and on the time step). In the specific case shown in the illustrative example (Figs. 8 and 9), we have taken up to 15 harmonics which are the most representative in magnitude.

B. Wavelets

The wavelet transform (WT) is a mathematical tool [55]–[57], similar to the Fourier Transform, that decomposes a signal into different scales with different levels of resolution by dilating a single prototype function. The decomposition into scales is made possible based on the fact that the wavelet transform is based on a square-integrable function and group theory representation. The wavelet transform, provides a local representation (in both time and frequency domains) of a given signal. Therefore, it is suitable for analyzing a signal where time-frequency resolution is needed such as disturbance transition events in power-quality analysis.

The integral WT of $f(t)$ is defined by WT_f as [57]

$$WT_f = \int_{-\infty}^{\infty} f(t) w_{\alpha,\beta}(t) dt \tag{48}$$

where $w_{\alpha,\beta}$ is the basis function known as mother wavelet or window function, and takes the form

$$w_{\alpha,\beta}(t) = \frac{1}{\sqrt{|\alpha|}} w\left(\frac{t-\beta}{\alpha}\right). \tag{49}$$

The mother wavelet $w(t)$ is an oscillating and damped function. Each wavelet, $w_{b,a}(t)$ is a scaled (compressed or dilated) and translated (shifted) version of the same original function $w(t)$, α represents a time dilation (controls the wavelet frequency), and β is a time translation (gives the position of the wavelet), and $1/\sqrt{\alpha}$ is an energy normalization factor that keeps the energy of the scaled wavelets the same as the energy of the mother wavelet. The original function $f(t)$ can be recovered by

$$f(t) = \frac{1}{C_w} \int_{-\infty}^{\infty} \int_{-\infty}^{\infty} WT_f w_{\alpha,\beta}(\alpha) \frac{d\alpha}{\alpha^2} d\beta \tag{50}$$

where $\alpha > 0$, and the constant C_w is given by

$$C_w = \int_{-\infty}^{\infty} \frac{|W(\omega)|^2}{|\omega|} d\omega. \tag{51}$$

The mother wavelet determines the shape of the components of the decomposed signal. Wavelets must be oscillatory, decay at least as fast as $1/\sqrt{|\omega|}$ as $\omega \to \infty$, and have an average of zero. The most common types of wavelets are shown in Fig. 10.

Translating the mother wavelet continuously over a real continuous number system, generates substantial redundant information. Therefore, instead of continuous dilatation and translation, the mother wavelet must be dilated and translate discretely by selecting $\alpha = \alpha_o^m$ and $\beta = n\beta_o\alpha_o^m$ where α_o and β_o are fixed constants with $\alpha_o > 1$, $\beta_o > 0$, and m and n are positive integers. Then, the discretized mother wavelet becomes

$$w_{m,n}(t) = \alpha_o^{-m/2} w\left(\frac{t - n\beta_o\alpha_o^m}{\alpha_o^m}\right) \tag{52}$$

and the corresponding discrete wavelet transform (DWT) is given by

$$DWT_f(m,n) = \int_{-\infty}^{\infty} f(t) w_{m,n}(t) dt. \tag{53}$$

In the DWT, the original waveform is decomposed into an approximation and a detail at the first stage and then successive decompositions are performed on the approximation only with no further decomposition for the details, hence obtaining the multi-resolution analysis (MRA). Based on careful choice of the number of decomposition levels and suitable choice of the wavelet family, the problem of spectral leakage can be reduced. The number of levels depends on the harmonic order contained in the original waveform that is required to be calculated separately. Fig. 11 shows the coverage of the time-frequency plane for the wavelet and for the Fourier transform, the dimensions of

TABLE I
HYBRID TD–FD METHODOLOGIES

Technique	References	Application	Remarks
Harmonic power flow	[17] - [22]	Steady-state analysis	Used in a stand alone mode as an initialization procedure for electromagnetic transient programs
Harmonic balance	[23] - [33]	Steady-state analysis Harmonic analysis	Nonlinear elements solved in TD and linear elements in FD
Hybrid algorithm for transient stability	[34] - [38]	Power systems dynamics	Considerable reduction in computational time
Fault analysis	[39] - [41]	Fault analysis	Least square estimation algorithm as an interface
Full FD solution	[42] - [48]	Electromagnetic transient and steady-state analysis	Full FD solution, final FD solution variables are transformed into TD
Two zone hybrid solution	[49]	Electromagnetic transient analysis	Need a transmission line (delays) as a link between the two zones
NLT Hybrid Method for Steady and Dynamic States	[50]	Steady and dynamic state analysis	No need of resorting to iterative methods for the nonlinear part
Dynamic Harmonic Domain	[51] - [54]	Dynamic state analysis of harmonics and instantaneous waveforms	Allows tracking the behavior of harmonics (FD variables) with respect to time
Wavelets	[55] - [58]	Dynamic state analysis	Allows tracking the behavior of harmonics (FD variables) with respect to time

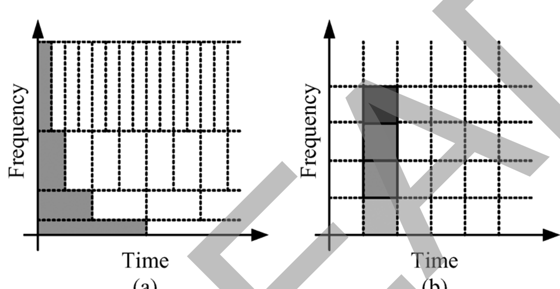

Fig. 11. Coverage of the time–frequency plane for: (a) the wavelet transform and (b) the Fourier transform.

the resolution squares represent minimum time and frequency intervals. Also from Fig. 11 one can notice that Fourier is restricted to a fixed window size while wavelets covers a wider frequency range [58].

VI. COMPARISON OF HYBRID TD–FD TECHNIQUES

Table I shows a brief comparison for hybrid techniques discussed before for easy visualization of citations, applications, and relevant remarks.

VII. CONCLUSION

The main purpose of this paper is to describe methods for interfacing frequency and time-domain techniques. Hybrid techniques have been classified into three categories: (a) steady-state: harmonic power flow and harmonic balance, (b) dynamic analysis for transient stability and fault calculations: synchronous machines in TD and the network in FD, and (c) electromagnetic transients: full FD or TD solution, and two-zone hybrid solution. A brief summary of the merits and limitations of the techniques are are presented.

The paper also presents a summary of the FD techniques used in power system analysis. Fourier, Hartley, Laplace, and z-transforms are, until now, the techniques that have been referenced to for power system analysis. Works with the Walsh and Mellin Transform had focused on signal filtering and relay protection. Discrete transforms of the methodologies presented are described as well.

In addition, two methodologies that have the capability to present results in time or frequency domain without postprocessing, are also presented. A brief summary of wavelets, including some classical wavelets, and the dynamic harmonic domain are discussed.

It is believed that this material will provide power system engineers with a sufficient background to understand the interfacing of TD and FD programs.

REFERENCES

[1] *The Authoritative Dictionary of IEEE Standards Terms Seventh Edition*, IEEE Std . 100, 2000.
[2] J. G. Proakis and D. G. Manolakis, *Digital Signal Processing: Principles, Algorithms, and Applications*. Englewood Cliffs, N J: Prentice-Hall, 1996.
[3] S. Qian and D. Chen, “Joint time-frequency analysis,” *IEEE Signal Process. Mag*, vol. 16, no. 2, pp. 52–67, Mar. 1999.

[4] R. N. Bracewell, *The Hartley Transform*. Oxford, U.K.: Oxford Univ. Press, 1986.

[5] E. Acha, J. J. Rico, S. Acha, and M. Madrigal, "Harmonic modelling in Hartley's domain with particular reference to three phase thyristor-controlled reactors," *IEEE Trans. Power Del.*, vol. 12, no. 4, pp. 1622–1628, Oct. 1997.

[6] G. T. Heydt, K. J. Olejniczak, R. Sparks, and E. Viscito, "Application of the Hartley transform for the analysis of the propagation of nonsinusoidal waveforms in power systems," *IEEE Trans. Power Del.*, vol. 6, no. 4, pp. 1862–1868, Oct. 1991.

[7] D. J. Wilcox, "Numerical Laplace transformation and inversion," *Int. J. Elect. Eng. Educ.*, vol. 15, pp. 247–265, 1988.

[8] S. J. Day, N. Mullineux, and J. R. Reed, "Developments in obtaining transient response using Fourier transforms. Part I: Gibbs phenomena and Fourier integrals," *Int. J. Elect. Eng. Educ.*, vol. 3, pp. 501–506, 1965.

[9] S. J. Day, N. Mullineux, and J. R. Reed, "Developments in obtaining transient response using Fourier transforms. Part II: Use of the modified Fourier transform," *Int. J. Elect. Eng. Educ.*, vol. 4, pp. 31–40, 1966.

[10] S. J. Day, M. J. Battison, N. Mullineux, and J. R. Reed, "Developments in obtaining transient response using Fourier transforms. Part III: Global response," *Int. J. Elect. Eng. Educ.*, vol. 6, pp. 259–265, 1968.

[11] J. L. Walsh, "A closed set of normal orthogonal functions," *Amer. J. Math.*, vol. 45, no. 1, pp. 5–24, Jan. 1923.

[12] K. Olejniczak and G. T. Heydt, "A comparison of alternative transforms for electric power engineering applications," in *Proc. 22nd NAPS*, Oct. 1990, pp. 84–93.

[13] J. L. Shanks, "Computation of the fast Walsh-Fourier transform," *IEEE Trans. Comput.*, vol. C-18, no. 5, pp. 457–459, May 1969.

[14] J. R. Ragazzini and L. A. Zadeh, "Analysis of sampled data systems," *Trans. AIEE*, vol. 71, pt. II, pp. 225–234, 1952.

[15] T. Noda and A. Ramirez, "z-transform-based methods for electromagnetic transient simulations," *IEEE Trans. Power Del.*, vol. 22, no. 3, pp. 1799–1805, Jul. 2007.

[16] A. V. Oppenheim, R. W. Schafer, and J. R. Buck, *Discrete-Time Signal Processing*, 2nd ed. Englewood Cliffs, NJ: Prentice-Hall, 1999.

[17] D. Xia and G. T. Heydt, "Harmonic power flow studies part I-formulation and solution," *IEEE Trans. Power App. Syst.*, vol. PAS-101, no. 6, pp. 1257–1265, Jun. 1982.

[18] D. Xia and G. T. Heydt, "Harmonic power flow studies part II-Implementation and practical application," *IEEE Trans. Power App. Syst.*, vol. PAS-101, no. 6, pp. 1266–1270, Jun. 1982.

[19] A. Semlyen, E. Acha, and J. Arrillaga, "Newton type algorithm for the harmonic phasor analysis ofnonlinear power sistems in periodical steady state with especial reference to magnetic nonlinearities," *IEEE Trans. Power Del.*, vol. 3, no. 3, pp. 1090–1098, Jul. 1988.

[20] B. K. Perkins, J. R. Marti, and H. W. Dommel, "Nonlinear elements in the EMTP: Steady-state initialization," *IEEE Trans. Power Syst.*, vol. 10, no. 2, pp. 593–601, May 1995.

[21] Q. Wang and J. R. Marti, "A waveform relaxation technique for steady state initialization of circuits with nonlinear elements and ideal diodes," *IEEE Trans. Power Del.*, vol. 11, no. 3, pp. 1437–1443, Jul. 1996.

[22] G. Murere, S. Lefebvre, and X. D. Do, "A generalized harmonic balance method for EMTP initialization," *IEEE Trans. Power Del.*, vol. 10, no. 3, pp. 1353–1359, Jul. 1995.

[23] S. R. Naidu and B. A. Souza, "Analysis of ferroresonant circuits in the time and frequency domains," *IEEE Trans. Magn.*, vol. 33, no. 5, pp. 3340–3342, Sep. 1997.

[24] S. R. Naidu and B. A. Souza, "Analysis of ferroresonant circuits using a Newton-Raphson scheme," *IEEE Trans. Power Del.*, vol. 12, no. 4, pp. 1793–1798, Oct. 1997.

[25] Y. Hu, X. Duan, and K. Mayaram, "A comparison of time-domain and harmonic balance steady-state analyses for coupled device and circuit simulation," in *Proc. 2nd Annu. IEEE Northeast Workshop on Circuits and Systems*, Jun. 2004, pp. 93–96.

[26] K. L. Lian and P. W. Lehn, "Steady-state solution of a voltage-source converter with full closed loop control," *IEEE Trans. Power Del.*, vol. 21, no. 4, pp. 2071–2081, Oct. 2006.

[27] A. Medina, "Harmonic simulation techniques (methods & algorithms)," in *Proc. IEEE Power Eng. Soc. General Meeting*, Jun. 2004, vol. 1, pp. 762–765.

[28] S. K. Chakravarthy and C. V. Nayar, "Parallel quasi-periodic ferroresonant oscillations in electrical power systems," *IEEE Trans. Circuits Syst. I: Fundam. Theory Appl.*, vol. 42, no. 9, pp. 530–534, Jul. 1995.

[29] A. Semlyen and M. Shlash, "Principles of modular harmonic power flow methodology," *Proc. Inst. Elect. Eng., Gen., Transm. Distrib.*, vol. 147, no. 1, pp. 1–6, Jan. 2000.

[30] M. Shlash and A. Semlyen, "Efficiency issues of modular harmonic power flow," *Proc. Inst. Elect. Emg., Gen., Transm. Distrib.*, vol. 148, no. 2, pp. 123–127, Mar. 2001.

[31] W. Wiechowski, J. Lykkegaard, B. Bank-Jensen, and C. Leth Bak, "Hybrid time/frequency domain modelling of nonlinear components," in *Proc. 9th Int. Conf. Electrical Power Quality and Utilisation*, Oct. 2006, pp. 1–6.

[32] A. Semlyen and A. Medina, "Computation of the periodic steady state in systems with nonlinear components using a hybrid time and frequency domain methodology," *IEEE Trans. Power Syst.*, vol. 10, no. 3, pp. 1498–1504, Aug. 1995.

[33] M. A. Moreno and J. Usaola, "Three-phase harmonic load flow in frequency and time domains," *Proc. Inst. Elect. Eng., Elrct. Power Appl.*, vol. 150, no. 3, pp. 295–300, May 2003.

[34] T. J. Bedford and A. G. Jack, "A method to compute transients in synchronous generators using frequency domain methods," *IEEE Trans. Energy Convers.*, vol. 3, no. 2, pp. 367–374, Jun. 1988.

[35] P. E. Crouch, E. Brady, and D. J. Tylavsky, "Frequency domain transient stability simulation of power system: Implementation by supercomputer," *IEEE Trans. Power Syst.*, vol. 6, no. 1, pp. 51–58, Feb. 1991.

[36] J. J. Sanchez-Gasca and J. H. Chow, "Performance comparison of three identification methods for the analysis of electromechanical oscillations," *IEEE Trans. Power Syst.*, vol. 14, no. 3, pp. 995–1002, Aug. 1999.

[37] D. R. Ostojic and G. T. Heydt, "Transient stability assessment by pattern recognition in the frequency domain," *IEEE Trans. Power Syst.*, vol. 6, no. 1, pp. 231–237, Feb. 1991.

[38] D. R. Ostojic and G. T. Heydt, "Real-time digital simulator with digital/analog conversion interface for testing power instruments," in *Proc. Power Industry Computer Application Conf.*, May 1993, pp. 336–342.

[39] S. M. Halpin, L. L. Grigsby, C. A. Gross, and R. M. Nelms, "An improved fault analysis algorithm for unbalance multi-phase power distribution systems," *IEEE Trans. Power Del.*, vol. 9, no. 3, pp. 1332–1338, Jul. 1994.

[40] S. M. Halpin, C. A. Gross, and L. L. Grigsby, "An improved method of including detailed synchronous machine representations in large power system models for fault analysis," *IEEE Trans. Energy Convers.*, vol. 8, no. 4, pp. 719–725, Dec. 1993.

[41] S. M. Halpin and R. F. Burch, "An improved simulation approach for the analysis of voltage flicker and the evaluation of mitigation strategies," *IEEE Trans. Power Del.*, vol. 12, no. 3, pp. 1285–1291, Jul. 1997.

[42] P. Moreno, R. Rosa, and J. L. Naredo, "Frequency domain computation of transmission line closing transients," *IEEE Trans. Power Del.*, vol. 6, no. 1, pp. 275–281, Jan. 1991.

[43] J. L. Naredo, J. A. Gutierrez, F. A. Uribe, J. L. Guardado, and V. H. Ortiz, "Frequency domain methods for electromagnetic transient analysis," in *Proc. IEEE Power Eng. Soc. General Meeting*, Jun. 2007, pp. 1–7.

[44] P. Moreno and A. Ramirez, "Implementation of the numerical Laplace transform: A review," *IEEE Trans. Power Del.*, vol. 23, no. 4, pp. 2599–2609, Oct. 2008.

[45] D. Crevier and F. C. Schweppe, "The use of Laplace transforms in the simulation of power system frequency transients," *IEEE Trans. Power App. Syst.*, vol. PAS-94, no. 2, pp. 236–241, Apr. 1975.

[46] W. D. Humpage, K. P. Wong, T. T. Nguyen, and D. Sutanto, " z-transform electromagnetic transients analysis in power systems," *Proc. Inst. Elect. Eng. C*, vol. 127, no. 6, pp. 370–378, Nov. 1980.

[47] W. D. Humpage, K. P. Wong, and T. T. Nguyen, "Development of z-transform electromagnetic transients analysis methods for multimode power networks," *Proc. Inst. Elect. Eng. C*, vol. 127, no. 6, pp. 379–385, Nov. 1980.

[48] M. M. Saied and A. Al-Fuhaid, "Electromagnetic transients in a line-transformer cascade by numerical Laplace transform technique," *IEEE Trans. Power Del.*, vol. PAS-140, no. 10, pp. 2901–2909, Oct. 1985.

[49] A. Semlyen and M. R. Iravani, "Frequency domain modeling of external systems in an electro-magnetic transients program," *IEEE Trans. Power Syst.*, vol. 8, no. 2, pp. 527–533, May 1993.

[50] A. Ramirez, "Frequency domain computation of steady and dynamic states including nonlinear elements," *IEEE Trans. Power Del.*, paper TPWRD-00468-2008, accepted for publication.

[51] J. J. Rico, M. Madrigal, and E. Acha, "Dynamic harmonic evolution using the extended harmonic domain," *IEEE Trans. Power Del.*, vol. 18, no. 2, pp. 587–594, Apr. 2003.

[52] A. Ramirez, A. Semlyen, and R. Iravani, “Harmonic domain characterization of the resonant interaction between generator and transmission line,” *IEEE Trans. Power Del.*, vol. 20, no. 2, pt. 2, pp. 1753–1762, Apr. 2005.

[53] J. J. Chavez and A. Ramirez, “Dynamic harmonic domain modeling of transients in three-phase transmission lines,” *IEEE Trans. Power Del.*, vol. 23, no. 4, pp. 2294–2301, Apr. 2008.

[54] T. Noda, A. Semlyen, and R. Iravani, “Entirely harmonic domain calculation of multiphase nonsinusoidal steady state,” *IEEE Trans. Power Del.*, vol. 19, no. 3, pp. 1368–1377, Jul. 2004.

[55] A. Haar, “Zur Theorie der orthogonalen Funktionensysteme,” *Math. Annal.*, no. 3, pp. 331–371, 1910.

[56] A. Graps, “An introduction to wavelets,” *IEEE Comput. Sci. Eng.*, vol. 2, no. 2, pp. 50–61, Spring 1995.

[57] A. Cohen and J. Kovacevic, “Wavelets: the mathematical background,” *Proc. IEEE*, vol. 84, no. 4, pp. 514–522, Apr. 1996.

[58] O. Rioul and M. Vetterli, “Wavelets and signal processing,” *IEEE Signal Process. Mag.*, vol. 8, no. 4, pp. 14–38, Oct. 1991.

[59] B. Gustavsen, “Validation of frequency-dependent transmission line models,” *IEEE Trans. Power Del.*, vol. 20, no. 2, pt. 1, pp. 925–933, Apr. 2005.

[60] A. M. Youssef, T. K. Abdel-Galil, E. F. El-Saadany, and M. M. A. Salama, “Disturbance classification utilizing dynamic time warping clasiffier,” *IEEE Trans. Power Del.*, vol. 19, no. 1, pp. 272–278, Jan. 2004.